Structural phase transitions in the perovskite-type layer compounds $NH_3(CH_2)_3NH_3CdCl_4$, $NH_3(CH_2)_4NH_3MnCl_4$, and $NH_3(CH_2)_5NH_3CdCl_4$

R. Kind, S. Plesko, and P. Günter
Laboratory of Solid State Physics, Swiss Federal Institute of Technology, Hönggerberg, CH-8093 Zürich, Switzerland

J. Roos
Institute of Physics, University of Zürich, CH-8001 Zürich, Switzerland

J. Fousek
Institute of Physics, Czechoslovak Academy of Sciences, Prague 8, Czechoslovakia
(Received 29 October 1980)

The structural phase transitions in the perovskite-type layer-structure compounds $[NH_3(CH_2)_3NH_3]CdCl_4$ ($T_c = 375$ K), $[NH_3(CH_2)_4NH_3]MnCl_4$ ($T_c = 382$ K), and $[NH_3(CH_2)_5NH_3]CdCl_4$ ($T_c = 338$ K) have been studied by ^{35}Cl and deuteron quadrupole resonance spectroscopy, birefringence, and dilatation measurements, optical-domain investigations and group-theoretical considerations. The results show that this transition, which is for all three compounds of second order, is basically a dynamic order-disorder transition of the alkylenediammonium chains, each of which can take on four different states (two all-trans states and two twisted states). The high-temperature phase is characterized by a dynamical disorder of the chains between the four possible states, the twisted states being less populated because of their higher potential energy. In the low-temperature phase, well below the phase transition, the chains are completely ordered in one of the two all-trans states. A strong even-odd effect, concerning the number of carbon atoms in the alkylene chains, has been observed in the temperature dependence of the static dielectric constant and in the critical exponent β of the order parameter. This is connected with the symmetry of the chains in the all-trans state which is $mm2$ for "odd" chains and $2/m$ for "even" chains. In contrast to the "even" chains the "odd" chains can thus carry a permanent electric dipole moment. As a consequence the phase transition in the two Cd compounds is of antiferrodistortive nature and leads from a paraelectric phase to an antiferroelectric phase, whereas the Mn compound undergoes a proper ferroelastic transition, although the microscopic mechanism is the same for both types. It is shown that the order-disorder transition in these compounds can be described adequately with a microscopic rigid-lattice model in the mean-field approximation.

I. INTRODUCTION

Structural phase transitions in perovskite-type layer compounds have gained much interest in the past five years. Many studies of substances of the formula $(C_nH_{2n+1}NH_3)_2MCl_4$ (so called monoammonium series), $M = Cd,Mn$, have been published. They showed that structural changes in these compounds are a result of an interplay between a planar system of corner-sharing Cl octahedra and motions of the alkylammonium chains located between adjacent octahedral planes.[1–16] For chains with $n \geq 4$, structural rearrangement due to conformational changes of the chains becomes important.[17–23] Structural phase transitions are also reported for $[NH_3(CH_2)_nNH_3]MCl_4$-type materials (diammonium series) in which the link between adjacent octahedral planes is performed by alkylene chains bearing NH_3 groups on both ends.[7,24–30] Several structure determinations on compounds of this second class of layer perovskites have been performed: $[NH_3(CH_2)_2NH_3]MCl_4$, $M = Cu$,[31,32] $M = Mn$,[32] $M = Cd$,[33] $[NH_3(CH_2)_3NH_3]MCl_4$, $M = Mn$,[24,34] $M = Fe$,[34] $M = Cd$,[33,35] $[NH_3(CH_2)_4NH_3]MCl_4$, $M = Mn$,[30] $M = Cd$,[33] $[NH_3(CH_2)_nNH_3]MCl_4$, $M = Cd, n = 5–8$.[33] All these materials show essentially the same structure but in contrast to the monoammonium compounds the MCl_6 octahedra of adjacent planes are situated on top of each other and are not shifted by half a lattice constant. Figure 1 shows the room-temperature structure $P2_1/b$ of $[NH_3(CH_2)_4NH_3]MnCl_4$ according to Ref. 30.

The aim of the present work was the characterization of the structural phase transitions in $[NH_3(CH_2)_nNH_3]MCl_4$ as a function of the number n of CH_2 groups in the alkylene chains. For this pur-

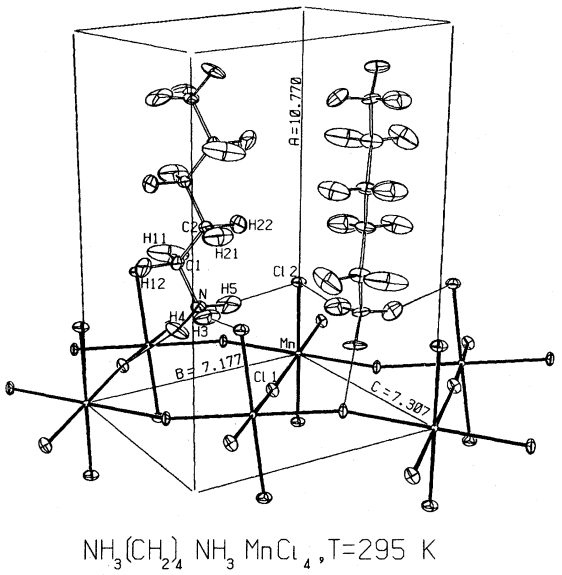

FIG. 1. View of the unit-cell content of $NH_3(CH_2)_4NH_3MnCl_4$ in the monoclinic low-temperature phase showing the ordered organic chains and one $MnCl_4$ layer. Hydrogen bonds are shown as light lines (after Ref. 30).

pose we have chosen the three compounds $[NH_3(CH_2)_3NH_3]CdCl_4$, $[NH_3(CH_2)_4NH_3]MnCl_4$, and $[NH_3(CH_2)_5NH_3]CdCl_4$ (henceforth designated as $2C_3Cd$, $2C_4Mn$, $2C_5Cd$), since they all undergo second-order phase transitions. Unfortunately in both the Cd series and the Mn series there are members undergoing strong first-order phase transitions, i.e., $[NH_3(CH_2)_3NH_3]MnCl_4$ (Ref. 24) and $[NH_3(CH_2)_4NH_3]CdCl_4$ (Refs. 26, 27, and 33). Since the MCl_6 octahedra have almost the same size for Mn and Cd, a comparison of the phase transitions is still reasonable. The compounds with $n=2$ show no structural phase transitions at all up to the decomposition temperature: $M=$Cd,[26] $M=$Mn, Cu,[36] i.e., the $NH_3(CH_2)_2NH_3$ groups are ordered for the whole temperature range of existence of these compounds.

The investigations on $[NH_3(CH_2)_3NH_3]MnCl_4$ (Ref. 24) revealed a dynamical disorder of the alkylene chains between two equivalent orientations in the orthorhombic high-temperature phase. The chains are flipping around the long axis about an angle of approximately 70°. In the low-temperature phase this motion is "frozen in" and the chains are completely ordered in one of the two orientations. The same was observed for $2C_4Mn$,[3] but in addition to the two equivalent all-trans states of the chains in the disordered high-temperature phase, also twisted states of the chains have been observed by neutron scattering. For symmetry reasons these twisted states cannot be distinguished from the all-trans states by NMR-NQR (nuclear-magnetic-resonance–nuclear-quadrupole-resonance) measurements. In the completely ordered low-temperature phase of $2C_4Mn$ no twisted states of the chains were observed. As we shall see later on the same situation occurs in $2C_3Cd$ and $2C_5Cd$.

Measurements of the static dielectric constant revealed a drastic even-odd effect, i.e., there are considerable drops of ϵ below T_c in $2C_3Cd$ and $2C_5Cd$, whereas the dielectric constant is almost not affected by the phase transition in $2C_4Mn$.[1,26] ϵ is the dielectric constant parallel to the layers. It was shown that a possible permanent dipole moment lying in the trans planes of the odd alkylene chains parallel to the layers would lead to a low-temperature structure with a planewise antiparallel arrangement of moments, i.e., to an antiferroelectric phase.[1] Such a permanent dipole is not possible for a chain with an even number of carbon atoms since there exists a center of inversion $\bar{1}$ in the middle of the chain. We shall see that there are further even-odd effects in these compounds.

In Sec. II group-theoretical aspects of the phase transitions in $2C_3Cd$, $2C_4Mn$, and $2C_5Cd$ are considered. Section III contains NMR-NQR measurements and measurements of birefringence and dilatation, as well as the characterization of observed domains. In Sec. IV a microscopic mean-field theory including all-trans and twisted states of the chains is given.

II. GROUP-THEORETICAL CONSIDERATIONS

In order to compare the structural phase transitions in $2C_3Cd$, $2C_4Mn$, and $2C_5Cd$ it is convenient to assign the orthorhombic crystal axes such that the symmetry coordinates of the corresponding soft modes are similar for all three compounds. For $2C_4Mn$ the axes are defined by the notation *Pnmb* of the high-temperature space group D_{2h}^7 (No. 53).[30] In this notation a is the axis perpendicular to the layers and we have $a=10.690$, $b=7.218$ and $c=7.37$ Å and the number of formula units in the primitive unit cell is $Z=2$. In the low-temperature phase the space group is $P112_1/b$, C_{2h}^5 (No. 14) with $Z=2$, $a=10.770$, $b=7.117$, $c=7.307$ Å, and $\gamma=92.67°$. The soft mode of the corresponding phase transition transforms according to the Γ_3^+ representation of the point group *mmm*.[30] The transition temperature is $T_c=382$ K.

The high-temperature space group of $2C_3Cd$ and $2C_5Cd$ is D_{2h}^{28} (No. 74) with $Z=2$ and the correct setting of the crystal axes is achieved by the notation *Immb*. The low-temperature space group for both compounds is *Pmnb*, D_{2h}^{16} (No. 62) with $Z=4$. In this phase we have $a=19.007$, $b=7.239$, and $c=7.481$ Å for $2C_3Cd$ and $a=23.929$, $b=7.329$, and $c=7.501$ Å for $2C_5Cd$, respectively.[33] In contrast to $2C_4Mn$ the a-lattice constant contains two interlayer distances as a consequence of the odd number of carbon atoms in the alkylene chains. The soft mode of

the phase transition condenses at the X point of the orthorhombic body-centered Brillouin zone: $\vec{q}=\frac{1}{2}(\vec{g}_1-\vec{g}_2+\vec{g}_3)$. It transforms according to the X_4^+ representation of the point group *mmm*. The transition temperature is $T_c=375$ K for $2C_3Cd$ and $T_c=338$ K for $2C_5Cd$, respectively.

A tetragonal high-temperature phase as found in the monoammonium series was not observed in the diammonium series up to the decomposition temperature, although such a parent phase would be possible. The space group of this parent phase would be for all three compounds $P4/mmm$, D_{4h}^1 (No. 123) with $Z=1$. Because of the symmetry of the alkylene chains this structure would have to be of dynamical nature, i.e., the chains would perform reorientational jumps around the fourfold axis between four equivalent orientations. These four orientations correspond to potential wells owing to the coupling of the NH_3 groups to the MCl_4-octahedra matrix by weak N-H—Cl bonds (see Fig. 1). The matrix itself can have a static tetragonal structure. With a soft mode condensing at the R point ($2C_3Cd$, $2C_5Cd$) of the tetragonal Brillouin zone or at the M point ($2C_4Mn$), respectively, one obtains the truly existing orthorhombic high-temperature phases. The selection of these soft-mode q vectors is a consequence of the symmetry of alkylenediammonium chains in the all-trans conformation which is $mm2$ for an odd number of carbon atoms but $2/m$ for an even number of carbon atoms. The soft-mode eigenvector consists, for the octahedral matrix, of a wash-board-like tilting of the MCl_6 octahedra around the orthorhombic b axis (parallel to the layer) (Ref. 30). The only odd-even effect is that octahedra of adjacent layers situated on top of each other are rotated in the same sense for $2C_4Mn$, whereas they are rotated in the opposite sense for $2C_3Cd$ and $2C_5Cd$. These rotations have, of course, the full symmetry Γ_1^+ of the orthorhombic high-temperature phases. Considering the alkylenediammonium groups the structure is still of dynamic nature. The symmetry of the chains would allow a static structure but the orientation of the chains in the potential wells is violating the mirror plane $\{m_y/000\}$, which is present in *Immb* as well as in *Pnmb*. Thus these space groups describe the time average of the structures. Due to the tilting of the octahedra two out of the four potential wells of a rigid chain become energetically so much favored that the probability of finding the chain in the other two wells is practically zero. Thus the chain dynamics consists essentially of reorientational jumps between two equilibrium orientations separated by an angle of 70°. This was observed by means of deuteron NMR-NQR measurements (see next section) and in the case of $2C_4Mn$ also by neutron scattering.[30] On lowering the temperature below T_c this disordered structure becomes ordered, i.e., the chain motion freezes-in in one of the two potential wells.

The soft-mode eigenvector, i.e., the relevant linear combination of the symmetry coordinates corresponding to the representations X_4^+ and Γ_3^+, respectively, can be obtained by assuming rigid MCl_6 octahedra and rigid alkylenediammonium chains in the all-trans conformation. It consists essentially of rotations of the MCl_6 octahedra around the a axis (layer normal) as well as of rotations of the time-averaged trans planes of the chains around the a axis. Above T_c the occupation probabilities n_1 and n_2 of the two potential wells is equal ($n_1=n_2=\frac{1}{2}$), i.e., the time average of the trans planes coincides with the mirror plane $\{m_y/000\}$. Below T_c we have $n_1>n_2$ and the planes corresponding to the time-averaged orientation of the chains is inclined by an angle ϕ with respect to the mirror plane $\{m_y/000\}$ of the high-temperature phase and thus this symmetry element is lost. As long as the angle ϕ is small enough, it is directly proportional to the order parameter which can be defined as $\eta=n_1-n_2$. As we shall see later on, the angle ϕ can be measured by means of deuteron NMR-NQR.

Up to now we have treated the alkylenediammonium chains as rigid groups. This was justified by the ordered low-temperature phase where all chains are in the all-trans conformation. The neutron diffraction study,[30] however, showed the existence of twisted states in the orthorhombic high-temperature phase of $2C_4Mn$, i.e., states where the upper part of the chain has the orientation (1) whereas the lower part of the chain has the orientation (2). Thus each chain has four different states, two all-trans states and two twisted states. The twisted states are energetically unstable, as the torsion angle around the middle C—C bond is $52\pm10°$ and therefore near to the potential-energy maximum. The maximum, however, is rather low; for the butane chain in the gaseous state it is 12.3 kJ mol^{-1} only, and the energy necessary to adapt the twisted state can well be supplied by thermal motion in the crystal. A reason for having four different states of the chains in the high-temperature phase is the value of the transition entropy which is $\Delta S=1.17$ R for $2C_3Cd$, $\Delta S=0.97$ R for $2C_4Mn$, and $\Delta S=1.13$ R for $2C_5Cd$, respectively.[37] For a two-site rigid-lattice model with independent chains one would expect a value $\Delta S=R\ln2=0.69$ R, whereas a four-site model would yield $\Delta S=R\ln4=1.39$ R. In the low-temperature phase the twisted states are dying out so that well below the phase transition only all-trans states are left.

III. EXPERIMENTAL

A. Deuteron NMR-NQR measurements

As already mentioned above, alkylenediammonium chain motions play the most important part in the

structural phase transitions of perovskite layer compounds. For obtaining more detailed information concerning these phase transitions deuteron NMR-NQR measurements in the partially deuterated compounds $ND_3(CH_2)_nND_3MCl_4$ were performed. The crystal was placed in a large homogeneous magnetic field H_0 in such a way that H_0 can be rotated to take on all directions in the plane parallel to the octahedra layers. Resonance frequencies of the quadrupole perturbed Zeeman interaction of the deuteron nuclear-spin system were then measured as a function of the rotation angle. As a result one obtains a so-called rotation pattern from which information about the orientation of the electric field gradient (efg) tensor axes at the deuteron site relative to the crystal axes can be deduced. However, one does not obtain this information for each individual deuteron site, because several time-averaging processes are present.

First there is a rapid exchange of deuterons in a ND_3 group by jumpwise rotations about the threefold molecular axis. Hence, all three deuterons in a group see the same averaged efg tensor. Its largest principal axis points along the axis of hindered rotation, i.e., nearly parallel to the C–N bond terminating the hydrocarbon chain. The second averaging process is a flipping motion of the terminating CH_2ND_3 group of the chains around the a axis (which is perpendicular to the layers) between two stable orientations. Depending on the relative orientation of the two terminating CH_2ND_3 groups the chain is either in the all-trans state which has the lowest energy or it is in a twisted state. In the low-temperature phase well below the transition temperature the flipping motion is frozen in an all-trans state of the chains.[30]

Owing to these two processes we obtain from our deuteron rotation pattern directly the time-averaged directions of C–N bonds projected on to the layer plane. An example of such rotation pattern is shown in Fig. 2. Equivalent C–N bonds (or more precisely their corresponding ND_3 groups) show up as a pair of sinusoidal curves symmetrical with respect to the deuteron Larmor frequency ($\Delta\nu_Q=0$). The angular positions of maximum frequency splitting correspond to the situation where H_0 is parallel to the projection of the C–N bond on to the layer plane. In the low-temperature phases, where one of the two possible orientations is favored, we observe for all compounds two pairs of curves shifted by an angle 2ϕ with respect to each other.

Owing to the structure of the low-temperature phase the CH_2NH_3 groups of neighboring cavities have different orientations so that the time-averaged projections of the C-N directions on the layer plane differ by the angle 2ϕ. Approaching the transition temperature T_c from below, the angular shift 2ϕ gradually decreases until it reaches zero at $T \geq T_c$. At $T < T_c$ ϕ measures the deviation of the averaged C–N bond orientation from its angular position at

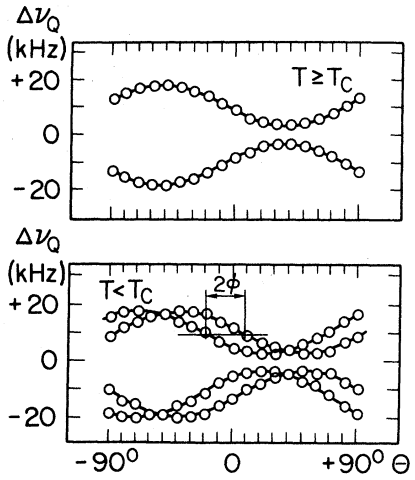

FIG. 2. Deuteron NMR-NQR rotation pattern of a single crystal of $ND_3(CH_2)_3ND_3CdCl_4$ for $\vec{H}_0 \perp a$. (Upper part $T \geq T_c$, lower part $T < T_c$.)

$T = T_c$ and is therefore directly related to the order parameter of this order-disorder transition. This relation is shown in Fig. 3. If we take n_1 or n_2 to be the probability for a N–C bond to have one of the two possible orientations, the order parameter η can be defined as $\eta = n_1 - n_2$. The averaged orientation of a C–N bond is represented by the position S of a center of gravity, $S = (n_1 - n_2)d$ and for ϕ we get the relation

$$tg\,\phi = (n_1 - n_2)\frac{d}{h} = \eta\, tg\,\phi_0 \ ,$$

or

$$\eta = tg\,\phi / tg\,\phi_0 \ . \qquad (1)$$

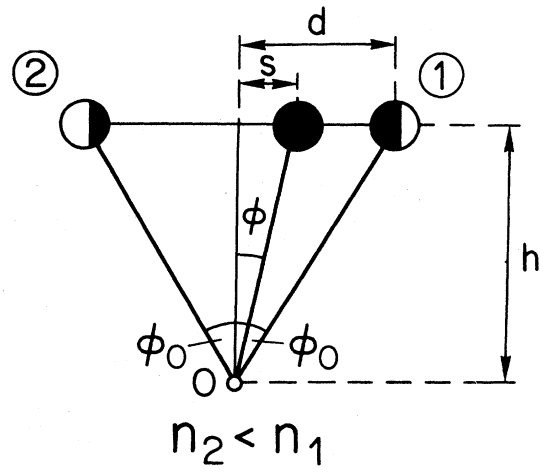

FIG. 3. Schematical representation of the relation between occupation probabilities of the two sites (1) and (2) and the angle ϕ describing the direction to the center of gravity of the two sites.

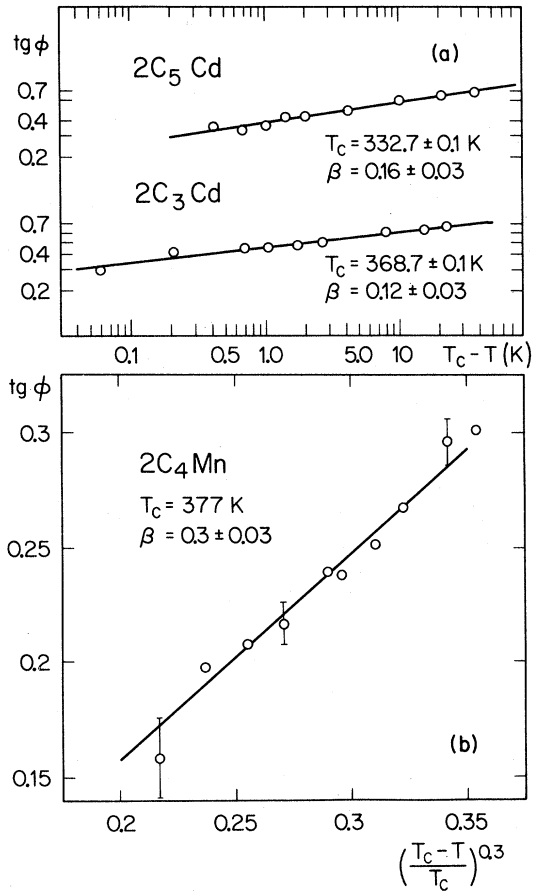

FIG. 4. Temperature dependence of $tg\,\phi$ for $ND_3(CH_2)_{3,5}ND_3CdCl_4$ (a) and $ND_3(CH_2)_4ND_3MnCl_4$ (b) plotted with suitable scales for the determination of the critical exponent β.

According to the formula

$$\eta = \text{const}[(T_c - T)/T_c]^{\beta} ,$$

we are able to determine the critical exponent β for these order-disorder transitions by simply measuring the temperature dependence of ϕ. To do this in a correct way one has to assume that ϕ_0 is not temperature dependent, at least in the neighborhood of T_c. This assumption is strongly supported by the neutron diffraction studies of the Mn compound.[30] The expression $[(T_c - T)/T_c]^{\beta}$ has been directly fitted to the measured values for $tg\,\phi$ and the results are shown in Figs. 4(a) and 4(b). In both Cd compounds ($n = 3, 5$) very low values for β around $\frac{1}{8}$ are obtained, whereas in the Mn compound we get a value in the neighborhood of $\frac{1}{3}$. This fact clearly shows that the transition behavior is strongly influenced by the odd-even effect mentioned above.

B. ^{35}Cl NQR measurements

Pure nuclear quadrupole resonance of ^{35}Cl nuclei is most attractive because the chlorine atoms occupy

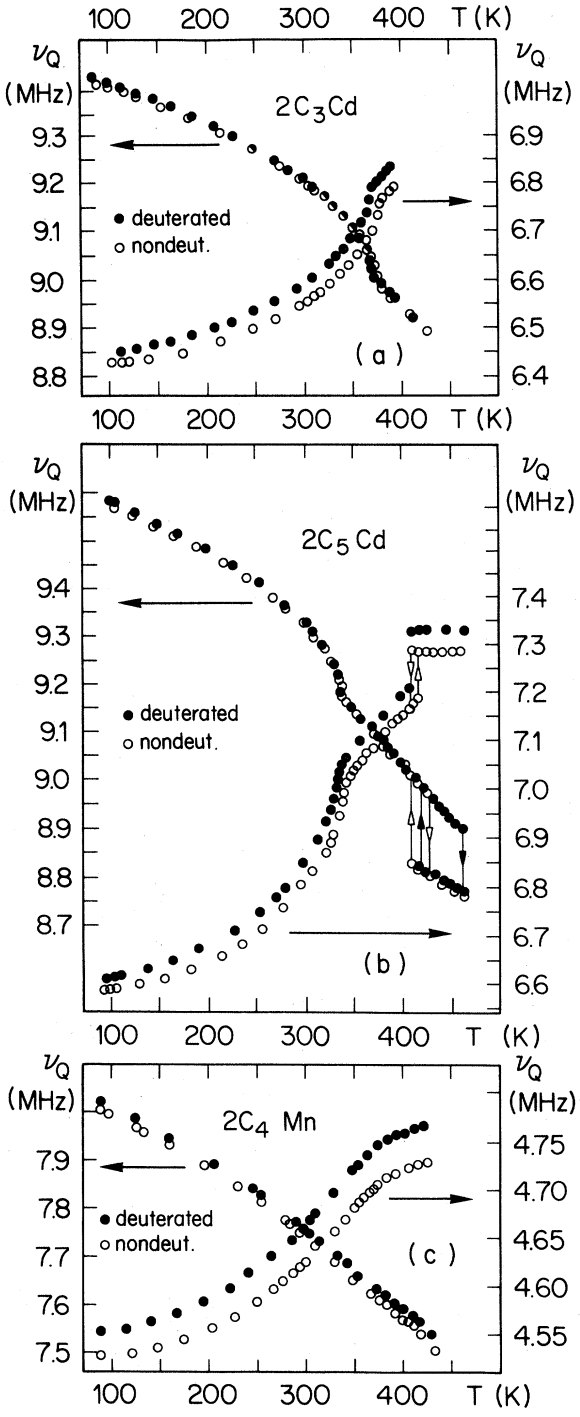

FIG. 5. Temperature dependence of the ^{35}Cl NQR frequencies of $NH_3(CH_2)_3NH_3CdCl_4$ (a), $NH_3(CH_2)_5NH_3CdCl_4$ (b), and $NH_3(CH_2)_4NH_3MnCl_4$ (c) and of the corresponding partially deuterated compounds. The NQR lines of the "bonding" chlorine atoms occur at higher frequencies than the lines of the "nonbonding" ones.

TABLE I. Transition temperatures and critical exponents deduced from the spontaneous change in $tg\phi \propto \eta$ and ^{35}Cl NQR.

Compound	T_c (K)	β	Chlorine site	μ	μ/β
$NH_3(CH_2)_3NH_3CdCl_4$	375	(0.12)	Bonding	0.47	(3.9)
			Nonbonding	...	
$ND_3(CH_2)_3ND_3CdCl_4$	370	0.12	*b*	0.46	3.8
			n	...	...
$NH_3(CH_2)_4NH_3MnCl_4$	382	(0.3)	*b*	...	...
			n	1.23	(4.1)
$ND_3(CH_2)_4ND_3MnCl_4$	377	0.3	*b*		...
			n	1.15	3.8
$NH_3(CH_2)_5NH_3CdCl_4$	340	(0.16)	*b*	...	...
			n	0.7	(4.4)
$ND_3(CH_2)_5ND_3CdCl_4$	333	0.16	*b*	...	...
			n	0.54	3.4

special sites in the octahedral matrix of the crystal. We can distinguish "bonding" chlorine sites due to corner sharing of MCl_6 octahedra and "nonbonding" sites above and below the metal ion plane. These two sites have different NQR frequencies ν_Q and can therefore be studied individually. Measurements of the temperature dependence of ν_Q have been performed in normal as well as in partially deuterated Cd and Mn compounds [Figs. 5(a),5(b),5(c)]. All frequencies are shifted to higher values in the partially deuterated compounds, the shift being more pronounced for "nonbonding" chlorine sites. By partial deuteration the transition temperature is lowered by approximately 6 K. As can be seen from Figs. 5(a),5(b),5(c) the NQR frequencies show a linear temperature dependence above T_c. Decreasing the temperature below T_c causes ν_Q to deviate continuously from the linear regime, thus displaying the second-order character of the transition. Remarkable is that the "bonding" chlorine site in the Mn compound seems to be unaffected by the transition. If we extrapolate the linear behavior of ν_Q to temperatures below T_c and subtract it from the effective values of ν_Q, we get the temperature dependence of the spontaneous frequency shift $\Delta\nu_Q$ for $T < T_c$. For temperatures not too far from T_c we introduce a critical exponent μ for $\Delta\nu_Q$ by assuming, that

$$\Delta\nu_Q \propto \left(\frac{T_c - T}{T_c}\right)^{\mu} . \tag{2}$$

Values for μ are then obtained by direct fitting of this expression to the measured values for $\Delta\nu_Q$. The relation between $\Delta\nu_Q$ and the order parameter η is simply given by

$$\Delta\nu_Q \propto \eta^{\mu/\beta} . \tag{3}$$

Values for the various exponents are summarized in Table I.

C. Domains at room temperature

For the room-temperature phase let us define: the *a* axis is perpendicular to the perovskite-like layers, and $b < c$. Platelets cut perpendicularly to the *a* axis are usually twinned, with domain walls having the orientations (011) or $(01\bar{1})$ when indexed with respect to the orthorhombic phase. Observations in polarized light show that in the neighboring domains the *b* and *c* axes are interchanged ("subtracting positions" differ by nearly 90°). Platelets perpendicular to the *b* or *c* axis reveal the same types of domain

walls. These facts together with the analogy to other layered perovskite structures allow one to conclude that the room-temperature phase may be considered to have resulted from a hypothetical parent phase with the point symmetry $4/mmm$, by a shear distortion $\pm u_{xy}$ (indexed in the tetragonal phase, i.e., with the z axis perpendicular to the layers).

In addition to the walls penetrating the whole volume of the sample, wedge-shaped domains can often be observed in the latter platelets. They are 2 to 15 μm thick at the edge of the sample, with diminishing thickness towards the opposite edge. Their presence causes a continuous change of the phase difference when traversing the sample in the direction or sudden jumps of the phase difference in the perpendicular direction.

The phase change $4/mmm$ to mmm is a ferroelastic transition and indeed switching may be induced by a uniaxial pressure applied perpendicularly to a. As expected, the mobility of wedge domains is higher than that of individual domain walls.

D. Refractive indices and birefringence at room temperature

The complete set of refractive indices at $T=300$ K and $\lambda=547$ nm measured with the minimum-deviation method are

$$n_a=(1.643\pm0.001),\quad n_c=(1.669\pm0.001)\ ,$$

$$n_b=(1.679\pm0.002)$$

for $2C_3Cd$ and

$$n_a=(1.579\pm0.002),\quad n_c=(1.601\pm0.001)\ ,$$

$$n_b=(1.611\pm0.001)$$

for $2C_5Cd$. (n_c for $2C_3Cd$ and n_a for $2C_5Cd$ are calculated by using the birefringence data.) Since $n_b>n_c>n_a$ the optical axes lie in the (ab) plane. At switching, the plane of optical axes rotates by 90°.

The dispersion of the refractive indices can be described by a single-term Sellmeier equation

$$n_i^2-1=\frac{S_2\lambda_i^2}{1-\lambda_i^2/\lambda^2}\ ,$$

where λ is the wavelength. Oscillator position λ_i and oscillator strength S_i are given in Table II.

The birefringence has been measured by using an Ehringhaus compensator. For $2C_3Cd$ at 300 K and for $\lambda=547$ nm we have found

$$\Delta_a n=n_b-n_c=+(94.3\pm1)\times10^{-4}\ ,$$

$$\Delta_c n=n_b-n_a=+(374.8\pm5)\times10^{-4}\ ,$$

$$\Delta_b n=n_c-n_a=+(283.5\pm5)\times10^{-4}\ .$$

Larger errors for $\Delta_b n$ and $\Delta_c n$ result from the uncertainty whether all wedge-shaped domains have been removed.

TABLE II. Sellmeier oscillator parameters derived from dispersion of refractive indices.

Material		S_i (10^{12} m^{-2})	λ_i (nm)
$2C_3Cd$	n_a	112	120
	n_c	96.6	132
$2C_5Cd$	n_c	93.3	126
	n_b	89.5	130

For $2C_5Cd$ under the same conditions:

$$\Delta_a n=(94.1\pm1)\times10^{-4}\ ,$$

$$|\Delta_c n|=(315.0\pm3)\times10^{-4}\ .$$

E. Phase transition in $2C_5Cd$ around 413 K

When the $2C_5Cd$ samples are heated up an additional phase transition occurs with a change of the point symmetry, as witnessed by a drastic rearrangement of the domain structure: the transition temperature is (413 ± 2) K where the 2-K limit indicates the scatter of transition temperatures for a number of samples and heating runs. On cooling, the symmetry returns to orthorhombic with a several-degrees hysteresis. This hysteresis proves the transition to be of 1st order. During the transition, the phase front is clearly visible under the microscope, its orientation being close to (001) for platelets parallel to a and (011) for platelets perpendicular to a.

Domain patterns in the upper phase are mostly very dense and complicated. In the rather scarce regions with larger domains one may identify extinction directions and domain-wall orientations. There exist regions with the original symmetrical extinctions as well as regions where the extinction directions are rotated by about ±24°. In the latter ones, observation in white light shows dispersion of the indicatrix axes. In addition to the original walls (100) and (010), indexed with respect to the hypothetical parent phase $4/mmm$, new boundaries (001) appear as well as such whose trace with the major surface of a plate parallel to c make an angle of about ±20° with the trace of a (001) boundary.

These and other detailed observations may all be explained by assuming the new high-temperature phase to be monoclinic. In analogy with other layered perovskite structures, the symmetry $2/m$ appears as most probable. Thus the observed domain struc-

TABLE III. Permissible domain walls in the monoclinic phase of $2C_5Cd$ (indexing with respect to the hypothetical tetragonal symmetry).

	D	C	B
A	(110), $(1\bar{1}\bar{f})$	$(1\bar{1}0)$, $(11f)$	(001), (010)
B	$(1\bar{1}0)$, $(11\bar{f})$	(110), $(1\bar{1}f)$	···
C	(001), (100)	···	

ture may be treated as resulting from a hypothetical transition $4/mmm$-$2/m$ where the twofold axis of the existing phase is perpendicular to the fourfold axis of the hypothetical phase and the mirror plane of the $2/m$ phase has tetragonal indices $(\bar{1}10)$ or (110). This transition generates four macroscopically distinguishable domains. We may describe one of them, denoted by A, by spontaneous deformations $u_{xx}, u_{yy}, u_{zz}, u_{yz}$ so that A is invariant with respect to the subgroup $2_x/m_x$ of the group $4/mmm$. Then the remaining domains may be characterized by the following twinning operations: $B \cdots 2_y$, $C \cdots 2_{\bar{x}y}$, $D \cdots 2_{xy}$. Table III gives the orientations of permissible walls (all tetragonal indexing) (Refs. 38 and 39).

The index f determining the orientation of some walls depends on the numerical value of the shear deformation and may be temperature dependent. In the orthorhombic phase the shear strains u_{yz}, u_{xz} vanish, $f=0$, and domains A and B as well as domains C and D become identical. In $2C_3Cd$ a similar transition is not observed up to 488 K.

F. Temperature dependence of the refractive indices and the birefringence

The temperature dependence of refractive indices n_a and n_c of $2C_3Cd$ and n_b, n_c of $2C_5Cd$ have been measured using the minimum-deviation method. The results of these measurements are plotted in Figs. 6 and 7. In the high-temperature phase of both compounds there is a linear temperature dependence for all the measured refractive indices. For $2C_3Cd$ the phase-transition-induced refractive index contributing to n_a and n_c is negative, whereas in $2C_5Cd$ this contribution is positive. Above the reconstructive phase transition in $2C_5Cd$ ($T_r = 413$ K) the refractive indices n_b and n_c both decrease with increasing temperature.

Temperature dependence of the path difference has been measured for mutually perpendicular cuts of $2C_3Cd$ by the Ehringhaus method. Figure 8 shows temperature dependences of normalized path differences Γ_a/l_0 and Γ_b/l_0, where $\Gamma_a = \Delta_a nl$, $\Gamma_b = \Delta_b nl$, l denoting the plate thickness whose room-temperature value is l_0. Thus at room temperature $\Gamma_a = \Delta_a n$, $\Gamma_b = \Delta_b n$.

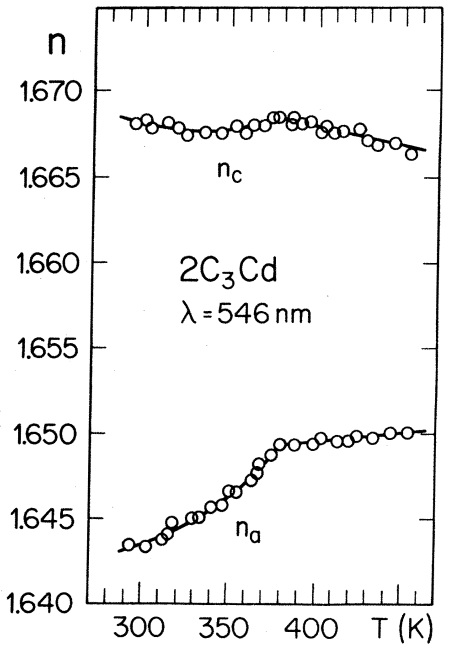

FIG. 6. Temperature dependence of refractive indices n_a and n_c for $2C_3Cd$.

The optical indicatrix suffers no rotation at the phase transition from *Pmnb* to *Immb*. Nevertheless, the transition manifests itself clearly in the Γ_i vs T curves by a sudden change of $d\Gamma_i/dT$ occurring at

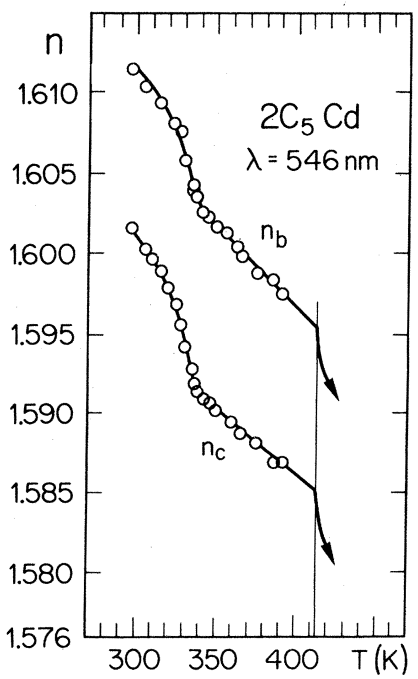

FIG. 7. Temperature dependence of refractive indices n_b and n_c for $2C_5Cd$.

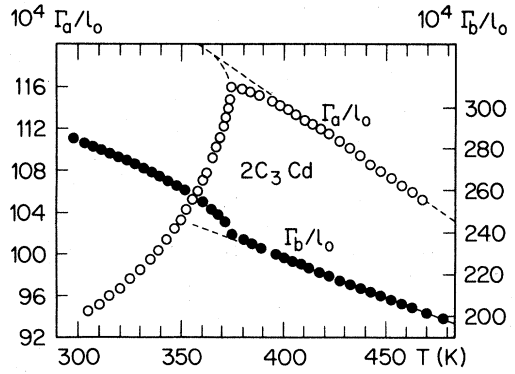

FIG. 8. Temperature dependence of the normalized path differences Γ_a/l_0 and Γ_b/l_0 for $2C_3Cd$.

$T_c = (375.3 \pm 0.3)$ K.

These data show the transition to be continuous. In the interference fringes, a jump of Γ_a should be clearly visible at the phase front if it were first order. It can be estimated that if such a jump exists it must be smaller than 1% of the $\delta_s\Gamma_a$ value at $T_c - 70$ K, where $\delta_s\Gamma_a$ is the change of the path difference induced by the transition.

Because of the possible presence of a wedge-shaped domain during the measurement of Γ_b/l_0, its temperature may be slightly distorted.

From the three quantities $\Gamma_a, \Gamma_b, \Gamma_c$, the Γ_a has the most pronounced change at T_c; it is determined by the value $\Delta_a n$ of birefringence within the perovskite sheets and by thermal dilatation occurring perpendicularly to the layers. Three distinct regions are seen in the $\Gamma_a(T)$ curve in Fig. 8. The linear dependence above 411 K can be held for the normal behavior of the parent phase. Between 411 K and T_c a significant departure from linear dependence occurs which can be thought of as a pretransition phenomenon caused by fluctuations of the order parameter η. The anomalous change below T_c is due to the onset of $\langle\eta\rangle$. In the last two regions, both $\Delta_a n$ and l may be coupled to $\langle\eta\rangle$ and its fluctuations. In order to find the true behavior of $\Delta_a n(T)$, a dilatometric study was made for an appropriate sample of $2C_3Cd$. A 3.3-mm-long rod with the major axis along the a direction was used; it was placed in the Linseis dilatometer and care was taken that the pressure of the quartz rod touching the sample was minimum. However, the domain structure in $2C_3Cd$ cannot be influenced by the stress σ_{xx} and even if there were a domain movement, it would not affect the dilatometric data since the u_{xx} strain in both domains is identical by symmetry.

Figure 9 shows the temperature dependence of the strain $u_{xx} = (l/l_0 - 1)$. Within the whole measured region, both below and above T_c, the thermal dilatation coefficient $\alpha_{xx} = du_{xx}/dT$ is negative. There is a pronounced anomaly of α_{xx} around T_c; some 15° above T_c, the departure from a linear dependence of

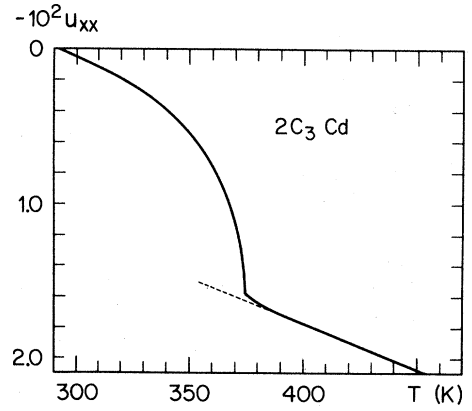

FIG. 9. Temperature dependence of the strain u_{xx} in $2C_3Cd$. ($u_{xx} = 0$ at $T = 293$ K by definition.)

u_{xx} vs T reveals again the effect of order-parameter fluctuations. These data have been used to evaluate the true $\Delta_a n(T)$ behavior from the Γ_a/l_0 curve. The result is shown in Fig. 10.

Comparing the curves of Γ_a/l_0 and $\Delta_a n$ vs T we see that the correction for thermal dilatation has caused only a minor modification. In the high-temperature region, the dependence is linear:

$$\Delta_a n = A + BT \quad , \tag{4}$$

with $A = 1.69 \times 10^{-2}$, $B = -1.31 \times 10^{-5}$ K^{-1}.

Spontaneous changes $\delta_s n$ of refractive indices caused by the onset of $\langle\eta\rangle$ must be proportional to $\langle\eta\rangle^{2}$.[40]

This follows from the fact that the transition is not ferroelastic (thus a linear dependence of $\delta_s n$ on $\langle\eta\rangle$ is forbidden) and that only changes of nondiagonal components of optical susceptibilities can couple, in the lowest order, to $\langle\eta\rangle^n$ with $n > 2$. Thus in our case $\delta_s n$ couples quadratically to η and therefore it is also sensitive to the fluctuations $\delta\eta$ of η.

In the parent phase we may thus write

$$\Delta_a n = A + BT + C\langle\delta\eta^2\rangle \tag{5}$$

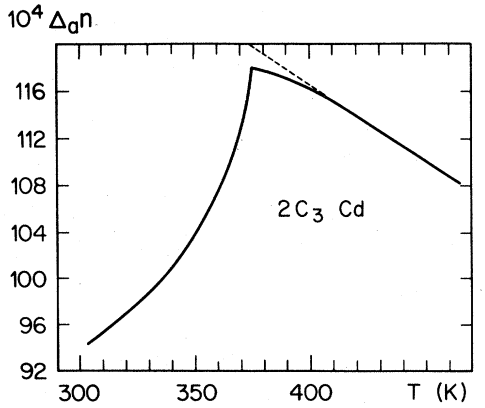

FIG. 10. Temperature dependence of the birefringence $\Delta_a n = n_b - n_c$ of $2C_3Cd$.

and our data show that the fluctuation term $C\langle\delta\eta^2\rangle$ plays a role between T_c and T_c+40 K. In the distorted phase we shall have

$$\Delta_a n = A + BT + \delta_s\Delta_a n \ , \tag{6}$$

where

$$\delta_s\Delta_a n = C(\langle\eta\rangle^2 + \langle\delta\eta^2\rangle) \tag{7}$$

is the "spontaneous" change of birefringence.

Due to the $\langle\delta\eta^2\rangle$ term, the birefringence measurements are not suitable for determining the critical coefficient in this and similar materials. The situation is different in proper ferroelastics where $\delta_s\Delta n \sim \langle\eta\rangle$ and close to T_c both $\delta_s\Delta n$ and η_s will have the same critical exponent.[41]

In the deuterated isomorph of $2C_3Cd$ (see Sec. III A) $\langle\eta\rangle$ has been measured using NMR and found to satisfy the law

$$\langle\eta\rangle \sim (T_c - T)^{0.12} \tag{8}$$

between $(T_c-0.06)$ K and (T_c-23) K. If there were no fluctuation contribution to $\delta_s\Delta_a n$ in the distorted phase, we would therefore expect

$$\delta_s\Delta_a n \sim (T_c - T)^{0.24} \tag{9}$$

in the same interval of temperatures. Knowing, however, that the fluctuations do influence $\Delta_a n$ in the parent phase within some 40 K, we can expect a similar effect even below T_c, though in a narrower interval (since the generalized susceptibility below T_c hardens two times faster than above T_c). Thus Eq. (9) cannot in fact be expected to be satisfied.

We may evaluate $\delta_s\Delta_a n(T)$ as a difference between the straight line $A+BT$ and the measured $\Delta_a n(T)$ below T_c. Figure 11 shows a log-log representation of $\delta_s\Delta_a n$ vs (T_c-T). It is seen that close to T_c down to (T_c-6) K, no exponential law is satisfied: this is the interval where the term $C\langle\delta\eta^2\rangle$ is certain to play a role.

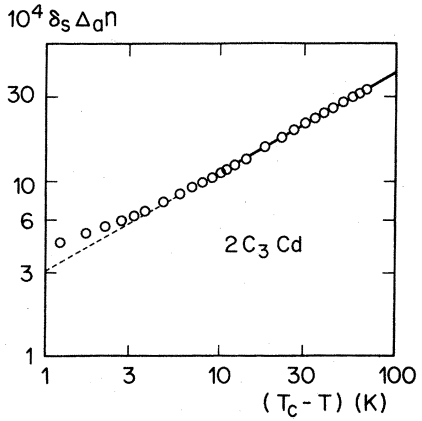

FIG. 11. Spontaneous birefringence $\delta_s\Delta_a n$ of $2C_3Cd$ vs T_c-T.

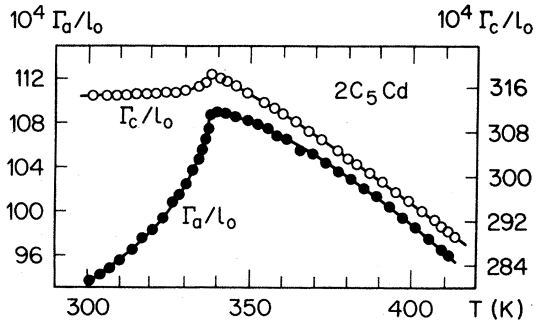

FIG. 12. Temperature dependence of the normalized path differences Γ_a/l_0 and Γ_c/l_0 for $2C_5Cd$.

Further below (T_c-6) K, we observe

$$\delta_s\Delta_a n = 3.19\times10^4(T_c - T)^{0.56} \ , \tag{10}$$

valid down to (T_c-70) K. No direct data on $\langle\eta\rangle$ are available in a correspondingly large interval which would test the proportionality $\delta_s\Delta_a n \sim \langle\eta\rangle^2$. Since this interval is rather far below T_c, it is possible that hard optical modes which are Raman active in the parent phase and condense in the distorted phase give a non-negligible contribution to $\delta_s\Delta_a n$, proportional to even powers of $\langle\eta\rangle$ higher than 2.

Although a more quantitative analysis of these data is at present not possible, it may be stated that the influence of order-parameter fluctuations on the refractive indices of $2C_3Cd$ is clearly established. By now it seems to be the largest observed effect in any material (cf., e.g., Hofmann's measurements on $BaTiO_3$).[42]

The data on $\Delta_b n(T)$ could be discussed in a similar way; however, here the spontaneous effect is smaller since n_a is obviously less influenced by the ordering of chains and the corresponding lattice distortion which occur mainly in the b-c plane.

Analogous measurements of path difference have

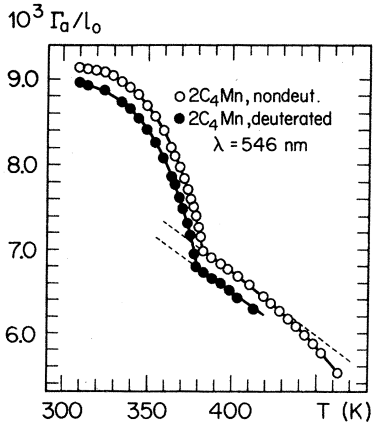

FIG. 13. Temperature dependence of the normalized path difference Γ_a/l_0 for partially deuterated and nondeuterated $2C_4Mn$.

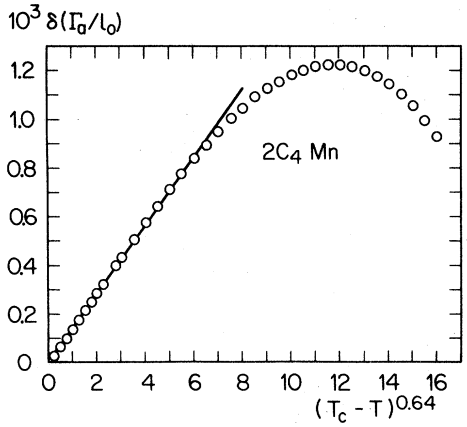

FIG. 14. Spontaneous birefringence $\delta_s\Delta_a n$ of $2C_4Mn$ vs $(T_c - T)^{0.64}$.

also been performed for $2C_5Cd$ and $2C_4Mn$ crystals. Figure 12 shows the temperature dependence of the normalized path differences in $2C_5Cd$. Complex twinning occurring in the monoclinic phase above 413 K prevents taking the data at higher temperatures. The behavior is rather similar to that of $2C_3Cd$. Here the transition occurs at $T_c = (337.9 \pm 0.3)$ K; optical observation verifies again its continuous character. The shape of the Γ_a/l_0 curve above T_c, namely, its increasing curvature when T_c is approached from above, manifests the appreciable fluctuation contribution to $\Delta_a n$ even in this compound.

The path difference Γ_a of both deuterated and undeuterated $2C_4Mn$ has been plotted in Fig. 13. In these compounds the phase transition occurs at $T_c = (378.2 \pm 0.5)$ K and $T_c = (381.9 \pm 0.3)$ K, respectively. Again, the optical observation verifies its continuous character. The spontaneous changes $\delta_s\Delta_a n$ of the birefringence have been plotted in Fig. 14. A few degrees below the $T_c = 381.9$ K $\delta_s\Delta_a n$ in undeuterated $2C_4Mn$ can be fitted best with

$$\delta_s\Delta_a n = b_0 + b_1(T_c - T)^{\beta'} + b_2(T_c - T)^{2\beta'} + b_3(T_c - T)^{3\beta'} , \quad (11)$$

with

$$\beta' = 0.65 , \quad b_0 = -0.01636 , \quad b_1 = +0.14289 ,$$

$$b_2 = 0.00146 , \quad b_3 = -0.000396 .$$

The fluctuation contribution $\Delta_a n$ in this compound is much smaller than in $2C_3Cd$ and $2C_5Cd$.

G. Sample preparation

$2C_3Cd$, $2C_5Cd$, and $2C_4Mn$ are all congruently soluble in aqueous solutions. Solubility data and crystal-growth procedures are adequately described in Ref. 43.

IV. MICROSCOPIC THEORY OF THE PHASE TRANSITIONS

In deriving the model Hamiltonian the following assumptions were made:

(a) The structural phase transitions are mainly due to the interactions among the alkylenediammonium chains. The MCl_4 layers within that approach are considered to be rigid matrices to which the NH_3 heads are linked. Any linear coupling between the chain motions and the phonons of the lattice just renormalizes the coupling constants.

(b) Each chain consists of two sections, each of which can have two stable orientations corresponding to a minimum in the potential energy, i.e., each chain has four different states. The two all-trans states are denoted by the indices $\alpha = 1, 2$ and the two twisted states by $\alpha = 3, 4$.

(c) The energy depends on the ratio of all-trans states and twisted states (since they have different potential energies), as well as of two-particle interactions between the chains. The two-particle interactions are of the intralayer type and of the interlayer type, describing the direct coupling between the chains, as well as the indirect coupling via the N-H—Cl bonds leading to bonding Cl sites. For a mean-field approximation (MFA) treatment it is, however, not necessary to distinguish between these interactions.

For the description of the Hamiltonian we used the largest unit cell of the system, i.e., the one of the orthorhombic low-temperature phase of $2C_3Cd$ with $Z = 4$ so that all transitions can be described by instabilities at the Brillouin-zone center ($q = 0$). In order to reduce the number of possibilities, it is assumed that the occupation probabilities n_α of the four states do not depend on the site of the chain in the unit cell. The assignment of the potential wells of the 4 chains in the unit cell was made in such a way that the observed low-temperature phases can be described by the frozen-in state of one chain only. Thus the frozen-in states $n_1 = 1$ or $n_2 = 1$ describe the two domains of the observed phases, i.e., the space groups $Pmnb$ ($2C_3Cd$, $2C_5Cd$) and $P112_1/b$ ($2C_4Mn$). A frozen-in twisted state $n_3 = 1$ or $n_4 = 1$ describes an ordered phase containing only twisted chains. Such a phase was observed in $2C_4Cd$.[33] The corresponding soft mode would condense at the Γ point of the orthorhombic body-centered Brillouin zone for the case of $2C_3Cd$ or at the X point of the orthorhombic primitive Brillouin zone for $2C_4Mn$.[30]

The mean-field Hamiltonian is obtained in the same way as shown in Ref. 10 for the case of $(CH_3NH_3)_2CdCl_4$. The n_α describe the occupation probabilities for the four states (α) of the chain. The single-particle energy U_1 is given by

$$U_1 = a(n_1 + n_2) + b(n_3 + n_4) , \quad (12)$$

where a and b are the potential energies of the all-trans states and twisted states, respectively. Taking the symmetry of the disordered high-temperature phase into account the two-particle interaction energy U_2 can be written as

$$U_2=\tfrac{1}{2}c'(n_1^2+n_2^2)+\tfrac{1}{2}c''(n_3^2+n_4^2)+d'(n_1n_2)+d''(n_3n_4)+e(n_1n_3+n_1n_4+n_2n_3+n_2n_4) \quad (13)$$

where c' and d' are the coefficients for trans-trans interaction, c'' and d'' the coefficients for twist-twist interaction, and e the coefficient for trans-twist interaction. The internal energy per one alkylenediammonium chain becomes $U=U_1+U_2$. The entropy per one chain is in the same approximation given by

$$S=-k[n_1\ln(n_1)+n_2\ln(n_2)+n_3\ln(n_3)+n_4\ln(n_4)] \quad (14)$$

and the corresponding free energy becomes $F=U-TS$, where T is the temperature. In view of the requirement $n_1+n_2+n_3+n_4=1$, we have to minimize the expression

$$F^*=F-\lambda(n_1+n_2+n_3+n_4-1) \quad , \quad (15)$$

where λ is the Lagrange multiplier. In equilibrium the first derivatives of F^* must vanish with respect to n, e.g.,

$$\frac{\partial F}{\partial n_1}=a+c'n_1+d'n_2+e(n_3+n_4)-\lambda+kT[\ln(n_1)+1]=0 \quad , \quad (16)$$

and all the eigenvalues of the matrix of the generalized inverse susceptibility $\chi^{-1}_{\alpha\beta}=\partial^2F/\partial n_\alpha\partial n_\beta$ have to be positive. For the disordered orthorhombic high-temperature phase we have $\langle n_1\rangle=\langle n_2\rangle\neq\langle n_3\rangle=\langle n_4\rangle$ and the matrix of the second derivatives of F^* has the following structure:

$$\frac{\partial^2F}{\partial n_\alpha\partial n_\beta}=\begin{pmatrix}A & C & E & E\\ C & A & E & E\\ E & E & B & D\\ E & E & D & B\end{pmatrix} \quad , \quad (17)$$

where $A=c'+kT/n_1$, $B=c''+kT/(\frac{1}{2}-n_1)$, $C=d'$, $D=d''$, $E=e$. The eigenvalues X_i of this matrix are given by

$$\begin{aligned}X_1&=A-C=c'-d'+kT/n_1 \quad ,\\ X_2&=B-D=c''-d''+kT/(\tfrac{1}{2}-n_1) \quad ,\\ X_3&=\tfrac{1}{2}\{A+B+C+D-[(A-B+C-D)^2+16E^2]^{1/2}\} \quad ,\\ X_4&=\tfrac{1}{2}\{A+B+C+D+[(A-B+C-D)^2+16E^2]^{1/2}\} \quad ,\end{aligned} \quad (18)$$

and the corresponding eigenvectors (representing deviations of the equilibrium occupation probabilities) are denoted by [1], [2], [3], and [4]

$$\begin{aligned}&[1]: \ \delta n_1=-\delta n_2, \ \ \delta n_3=\delta n_4=0 \quad ,\\ &[2]: \ \delta n_1=\delta n_2=0, \ \ \delta n_3=-\delta n_4 \quad ,\\ &[3]=[5]\cos(\theta/2)-[6]\sin(\theta/2) \quad ,\\ &[4]=[5]\sin(\theta/2)+[6]\cos(\theta/2) \quad ,\end{aligned} \quad (19)$$

where the vectors [5] and [6] are given by

$$\begin{aligned}&[5]: \ \delta n_1=\delta n_2=-\delta n_3=-\delta n_4 \quad ,\\ &[6]: \ \delta n_1=\delta n_2=\delta n_3=\delta n_4 \quad ,\end{aligned} \quad (20)$$

and where $tg\,\theta=4E/(A-B+C-D)$. The vector [6] is violating the condition $n_1+n_2+n_3+n_4=1$ and thus the system cannot become unstable with respect to the eigenvectors [3] and [4]. Therefore the only remaining eigenvectors are [1] and [2]. We can, however, introduce a parameter $\eta_5=n_1+n_2-n_3-n_4$, $-1<\eta_5<+1$ (corresponding to the vector [5]) which describes the ratio between all-trans states and twisted states. The disordered orthorhombic high-temperature phase is stable as long as the eigenvalues X_1 and X_2 are positive, i.e., as long as

$$\begin{aligned}T>T_1&=\frac{(-c'+d')(1+\eta_5)}{4k} \quad ,\\ T>T_2&=\frac{(-c''+d'')(1-\eta_5)}{4k} \quad .\end{aligned} \quad (21)$$

Below the temperature T_1 the system becomes unstable with respect to the eigenvector [1]. The corresponding order parameter η_1 can be defined as

$$\eta_1=n_1-n_2, \ \ -\frac{1+\eta_5}{2}<\eta_1<+\frac{1+\eta_5}{2} \quad . \quad (22)$$

In the same way we obtain for η_2

$$\eta_2=n_3-n_4, \ \ -\frac{1-\eta_5}{2}<\eta_2<+\frac{1-\eta_5}{2} \quad . \quad (23)$$

The disordered high-temperature phase is described by $\langle\eta_1\rangle=\langle\eta_2\rangle=0$, $-1<\eta_5<+1$, whereas the observed low-temperature phase is described by $\langle\eta_1\rangle\neq0$, $\langle\eta_2\rangle=0$, $\langle\eta_5\rangle>0$. In the ground state we have $\langle\eta_1\rangle=\pm1$, $\langle\eta_2\rangle=0$, $\langle\eta_5\rangle=+1$. The ordered phase which contains in the ground state only twisted chains is described by $\langle\eta_1\rangle=0$, $\langle\eta_2\rangle\neq0$, $\langle\eta_5\rangle<0$. In order to obtain the observed low-temperature phase the transition temperature T_1 must be higher than T_2

$$T_1>T_2\rightarrow-c'+d'>(-c''+d'')\frac{1-\eta_5}{1+\eta_5} \quad . \quad (24)$$

One can now express the free energy in terms of the

order parameters η_1, η_2, and η_5

$$F=\alpha\eta_5+\tfrac{1}{2}\beta\eta_1^2+\tfrac{1}{2}\gamma\eta_2^2+\tfrac{1}{2}\delta\eta_5^2+K$$
$$+\tfrac{1}{4}kT\{(1+2\eta_1+\eta_5)\ln[(1+2\eta_1+\eta_5)/4]$$
$$+(1-2\eta_1+\eta_5)\ln[(1-2\eta_1+\eta_5)/4]$$
$$+(1+2\eta_2-\eta_5)\ln[(1+2\eta_2-\eta_5)/4]$$
$$+(1-2\eta_2-\eta_5)\ln[(1-2\eta_2-\eta_5)/4]\}\ , \tag{25}$$

where

$$\alpha=\tfrac{1}{8}(4a-4b+c'-c''+d'-d'')\ ,$$
$$\beta=\tfrac{1}{2}(c'-d'),\quad \gamma=\tfrac{1}{2}(c''-d'')\ ,$$
$$\delta=\tfrac{1}{8}(c'+c''+d'+d''-4e)\ ,$$
$$K=\tfrac{1}{16}(8a+8b+c'+c''+d'+d''+4e)\ .$$

The free energy of the disordered high-temperature (HT) phase is

$$F_{\rm HT}=\alpha\eta_5+\tfrac{1}{2}\delta\eta_5^2+\tfrac{1}{2}kT\{(1+\eta_5)\ln[(1+\eta_5)/4]+(1-\eta_5)\ln[(1-\eta_5)/4]\}+K\ . \tag{26}$$

Since the entropy is zero for complete order, one obtains for the transition entropy for one mole of chains

$$\Delta S=-\frac{R}{2}\{(1+\eta_5)\ln[(1+\eta_5)/4]+(1-\eta_5)\ln[(1-\eta_5)/4]\}\ . \tag{27}$$

The value of η_5 at T_1 can thus be obtained from the measured transition entropies.[37]

$\eta_5(T_1)=0.62$ for $2C_3Cd$, $\eta_5(T_1)=0.84$ for $2C_4Mn$ and $\eta_5(T_1)=0.68$ for $2C_5Cd$, i.e., only about 18% of the chains are in a twisted state at the transition temperature. Using Eq. (21) one obtains the coefficient β

$$\beta=\tfrac{1}{2}(c'-d')=-\frac{2kT_1}{1+\eta_5}\approx-1.2kT_1\ . \tag{28}$$

The self-consistent equations for the order parameters $\langle\eta_1\rangle$ and $\langle\eta_5\rangle$ read

$$\frac{\partial F}{\partial\eta_1}=\beta\eta_1+\tfrac{1}{2}kT[\ln(1+2\eta_1+\eta_5)-\ln(1-2\eta_1+\eta_5)]=0\ , \tag{29}$$

$$\left.\frac{\partial F}{\partial\eta_5}\right|_{\langle\eta_2\rangle=0}=\alpha+\delta\eta_5+\tfrac{1}{4}kT[\ln(1+2\eta_1+\eta_5)+\ln(1-2\eta_1+\eta_5)-2\ln(1-\eta_5)]=0\ . \tag{30}$$

In the disordered high-temperature phase we have $\langle\eta_1\rangle=0$ and Eq. (29) is fulfilled for all values of η_5 and Eq. (30) reads

$$\alpha+\delta\eta_5+\tfrac{1}{2}kT\ln\frac{1+\eta_5}{1-\eta_5}=0\ . \tag{31}$$

Equation (31) describes a Boltzmann distribution between all-trans and twisted states of the chains for an energy difference 2α as long as the coefficient δ does not differ from zero. As one can see from Eq. (25), the coefficient α contains not only the single-particle energy difference $a-b$, but also the two particle interaction energies c', c'', d', and d''. There is, however, no reason for the coefficient δ to be equal to zero, so that we cannot expect a Boltzmann distribution of the states in the disordered high-temperature phase. Since we know the value of η_5 at $T=T_1$, Eq. (31) relates α and δ. For $2C_3Cd$ we get

$$\alpha=-0.725kT_1-0.62\delta\ . \tag{32}$$

Since the value of the coefficient β is already determined by Eq. (28), the coefficeint δ remains the only free parameter in the coupled equations (29) and (30). The solutions of these self-consistent equations are shown in Fig. 15 for three different values of δ. One can see that the symmetry-breaking order parameter $\langle\eta_1\rangle$ shows the usual mean-field behavior, whereas the spontaneous contribution of $\langle\eta_5\rangle$ is proportional to $\langle\eta_1\rangle^2$, since its critical exponent is equal to 1.0. The probability of finding a chain in the twisted state is equal to

$$\langle n_3\rangle+\langle n_4\rangle=(1-\langle\eta_5\rangle)/2\ . \tag{33}$$

Therefore its spontaneous contribution is also proportional to $\langle\eta_1\rangle^2$ near the transition temperature.

From the structure determination of $2C_4Cd$ (Ref. 33) (where the low-temperature phase contains only twisted chains) we know that the twisted chain is considerably shorter than the all-trans chain: $(l_{\rm trans}-l_{\rm twist})/l_{\rm trans}=0.07$. Therefore the interlayer distance and the corresponding lattice constant (a) strongly depends on the ratio of the two states. Since the NH_3 heads of the chains are only weakly bonded to the octahedra matrix it can safely be assumed that the mismatch between the actual interlayer distance and the length of a chain is corrected by a displacement of the NH_3 group in the a direction with respect to the equilibrium position in the octahedra matrix.

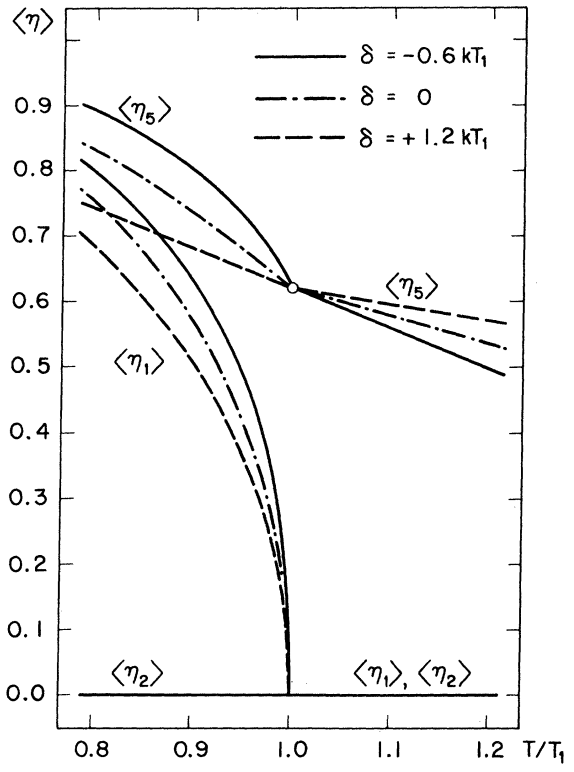

FIG. 15. Solution of the self-consistent equations for the order parameters $\langle\eta_1\rangle$, $\langle\eta_2\rangle$, and $\langle\eta_5\rangle$ of the rigid-lattice model for three different values of the coefficient δ.

For linear force constants one obtains for the strain in the a direction

$$u_{xx} = (l/l_0 - 1) = (\langle n_3\rangle + \langle n_4\rangle)(l_{\text{trans}} - l_{\text{twist}})/l_{\text{trans}} \sim 0.04(1 - \langle\eta_5\rangle) \quad . \tag{34}$$

The spontaneous strain u_{xx} should thus vary with the square of the order parameter $\langle\eta_1\rangle$ as already shown in Sec. III F. Introducing the calculated temperature dependence of $\langle\eta_5\rangle$ into Eq. (34) and comparing it with the measured strain (Fig. 9) a qualitative agreement between theory and experiment is obtained for both phases. Quantitative agreement can be reached in the high-temperature phase with $\delta = -0.6kT_1$, assuming that the strain values of $2C_4Cd$ (Ref. 33) can be adopted for the case of $2C_3Cd$. Since the measured critical exponent of the order parameter differs too much from the mean-field value no quantitative agreement can be reached in the low-temperature phase.

An interesting question is, how the experimental value of the energy difference ΔE between the all-trans state and the twisted state of a chain compares with the energy difference $b - a$ [Eq. (12)] introduced in our model. A value of $\Delta E = 12.3$ kJ/mol was measured for the twisted butane chain in the gaseous state.[44,45] For the case of $2C_3Cd$ this ΔE corresponds to $3.9kT_1$. Neglecting the two-particle interaction in the equation for the coefficient α [Eq. (25)] would give $\alpha \sim -2kT_1$. On the other hand, we obtain for the fitted value $\delta = -0.6kT_1$ via Eq. (32) $\alpha = -0.35kT_1$. However, if the twisted chain fits better into the structure than the all-trans chain, i.e., if it allows shorter N-H—Cl bonds, the difference in potential energy $b - a$ can be much smaller than ΔE of the gaseous state. Under this assumption the agreement between the measured and the theoretical value of α becomes much better.

V. CONCLUSIONS

From the above results, the following conclusions can be drawn:

(i) The second-order phase transitions in $2C_3Cd$, $2C_4Mn$, and $2C_5Cd$ can be basically described as order-disorder transitions of the $NH_3(CH_2)_nNH_3$ groups each of which has four possible equilibrium states: two all-trans states and two twisted states which differ in the mutual orientation of the upper and lower half-sections of the chains.

(ii) The twisted states have higher energy than the all-trans states and are therefore less populated in the disordered high-temperature phase. The transition entropy strongly depends on the population of the two states at the transition temperature.

(iii) Below the phase transition there is a spontaneous change in the ratio of the above-mentioned populations (favoring the all-trans states), which is proportional to the square of the order parameter. This has a direct influence on the spontaneous dilatation in the a direction, since the twisted chains are considerably shorter than the all-trans chains. This explains the negative temperature coefficient of both ordinary and spontaneous a dilatation.

(iv) The crystals show distinct pretransitional effects owing to the fluctuations of the order parameter $\langle\eta^2\rangle$. They are observed in the birefringence up to 40 K above T_c but not in the ^{35}Cl NQR. This is due to the fact that the NQR frequencies are well below the inverse correlation time τ_c^{-1} of the order-parameter fluctuations, whereas the optical frequencies are several orders of magnitude higher than τ_c^{-1}.

(v) The critical exponent β of the order parameter was measured from T_c down to $T_c - 20$ K to be $\beta = 0.12$ for $2C_3Cd$ and $\beta = 0.16$ for $2C_5Cd$, but $\beta = 0.3$ for $2C_4Mn$. This even-odd effect can well be due to the more-two-dimensional interaction between the permanent electric dipoles situated on the odd chains, which are responsible for the behavior of the dielectric constant. For symmetry reasons the even chains cannot carry a permanent dipole moment. Our MFA treatment of the phase transitions does not, of course, show this difference.

(vi) It is not evident why the spontaneous change

in the ^{35}Cl NQR frequencies is proportional to the fourth power of the order parameter, since the quadratic term is not forbidden for symmetry reasons. The quadratic terms can, of course, be cancelled by coincidence, but this effect, which was observed also in $(CH_3NH_3)_2MnCl_4$ for the bonding chlorine site, seems to have a deeper reason which is not understood at present. The same can be said for the critical exponent of the birefringence of $2C_3Cd$ and $2C_5Cd$ whereas the birefringence of $2C_4Mn$ varies with the square of the order parameter. But here even the linear term would be allowed since the transition is ferroelastic.

ACKNOWLEDGMENTS

The authors are very much indebted to H. Wüest, J. Mettler, and F. Rohner, ETH-Zürich, for technical assistance and for growth and preparation of crystals. They would like to thank also Dr. J. Havlicek, Czechoslovak Academy of Sciences, Prague, for the help in obtaining the dilatometric data. Moreover they would like to thank Professor B. Žekš, Institute Jozef Stefan, Ljubljana, for his critical comments on the first version of the theoretical part of the manuscript. This work was supported in part by the Swiss National Science Foundation.

[1]R. Kind, Ferroelectrics 24, 81 (1980).
[2]G. Chapuis, H. Arend, and R. Kind, Phys. Status Solidi A 31, 449 (1975).
[3]G. Heger, D. Mullen, and K. Knorr, Phys. Status Solidi A 31, 455 (1975).
[4]N. Lehner, K. H. Strobel, R. Geick, and G. Heger, J. Phys. C 8, 4096 (1975).
[5]J. Petzelt, J. Phys. Chem. Solids 36, 1006 (1975).
[6]R. Kind and J. Roos, Phys. Rev. B 13, 45 (1976).
[7]G. Chapuis, R. Kind, and H. Arend, Phys. Status Solidi A 36, 285 (1976).
[8]J. Seliger, R. Blinc, H. Arend, and R. Kind, Z. Phys. B 25, 189 (1976).
[9]M. Couzi, A. Daoud, and R. Perret, Phys. Status Solidi A 41, 271 (1977).
[10]R. Blinc, B. Zeks, and R. Kind, Phys. Rev. B 17, 3409 (1978).
[11]R. Kind, R. Blinc, and B. Zeks, Phys. Rev. B 19, 3743 (1979).
[12]R. Kind, Phys. Status Solidi A 44, 661 (1977).
[13]G. Chapuis, Acta Crystallogr. B 34, 1506 (1978).
[14]G. Chapuis, Phys. Status Solidi A 43, 203 (1977).
[15]W. Depmeier, Acta Crystallogr. B 33, 3713 (1977).
[16]R. Blinc, M. Burgar, B. Lozar, J. Seliger, J. Slak, V. Rutar, H. Arend, and R. Kind, J. Chem. Phys. 66, 278 (1977).
[17]M. Vacatello and P. Corradini, Gazz. Chim. Ital. 104, 773 (1974).
[18]M. Vacatello, Annu. Chim. 64, 13 (1974).
[19]V. Salerno, E. Landi, and M. Vacatello, Thermochim. Acta 20, 407 (1977).
[20]E. Landi and M. Vacatello, Thermochim. Acta 12, 141 (1975).
[21]M. A. Arrandiaga, M. J. Tello, J. Fernandez, H. Arend, and J. Roos, Phys. Status Solidi A 48, 53 (1978).
[22]R. Kind, S. Plesko, H. Arend, R. Blinc, B. Zeks, J. Slak, A. Levstik, C. Filipic, V. Zagar, G. Lahajnar, F. Milia, and G. Chapuis, J. Chem. Phys. 71, 2118 (1979).
[23]W. Depmeier and G. Chapuis, Acta Crystallogr. B 35, 1080 (1979).
[24]R. Kind, S. Plesko, and J. Roos, Phys. Status Solidi A 47, 233 (1978).
[25]H. Arend, K. Tichy, K. Baberschke, and F. Rys, Solid State Commun. 18, 999 (1976).
[26]A. Levstik, C. Filipic, R. Blinc, H. Arend, and R. Kind, Solid State Commun. 20, 127 (1976).
[27]R. Blinc, M. Burgar, B. Lozar, J. Seliger, J. Slak, V. Rutar, H. Arend, and R. Kind, J. Chem. Phys. 66, 278 (1977).
[28]M. J. Tello, M. A. Arrandiaga, and J. Fernandez, Solid State Commun. 24, 299 (1977).
[29]R. Kind, S. Plesko, and J. Roos, Helv. Phys. Acta 50, 601 (1977).
[30]K. Tichy, J. Benes, R. Kind, and H. Arend, Acta Crystallogr. B 36, 1355 (1980).
[31]G. B. Birrell and B. Zaslow, J. Inorg. Nucl. Chem. 34, 1751 (1972).
[32]K. Tichy, J. Benes, W. Hälg, and H. Arend, Acta Crystallogr. B 34, 2970 (1978).
[33]P. Walpen, Diploma Work (Institute for Crystallography, ETH Zürich, 1976) (unpublished).
[34]R. D. Willett and E. F. Riedel, Chem. Phys. 8, 112 (1975).
[35]R. D. Willett, Acta Crystallogr. B 33, 1641 (1977).
[36]H. Kammer, Helv. Phys. Acta 47, 442 (1975).
[37]A. Fouskova, Ferroelectrics 25, 451 (1980); and (private communication).
[38]J. Fousek, Czech. J. Phys. B 21, 955 (1971).
[39]J. Sapriel, Phys. Rev. B 12, 5128 (1975).
[40]J. Fousek and J. Petzelt, Phys. Status Solidi A 55, 11 (1979).
[41]J. Fousek, C. Konak, and G. Errandonea, J. Phys. C 12, 3197 (1979).
[42]R. Hofmann, S. H. Wemple, and H. Gränicher, J. Phys. Soc. Jpn. Suppl. 28, 265 (1970).
[43]H. Arend, W. Huber, F. H. Mischgofsky, and G. K. Richter van Leeuwen, J. Cryst. Growth 43, 213 (1978).
[44]W. Pechhold, Kolloid Z. Z. Polym. 228, 1 (1968).
[45]S. Weiss and G. E. Leroi, J. Chem. 48, 962 (1968).